Received: 1 July 2024 | Revised: 21 October 2024 | Accepted: 25 October 2024

https://doi.org/10.1016/j.rpth.2024.102618

ORIGINAL ARTICLE

In-depth characterization of *N*-glycosylation and sialic acid content in fetal and adult fibrinogen

Tana V. Palomino[1] | Anastasia Sheridan[2,3] | David C. Muddiman[1,3] | Ashley C. Brown[2,3]

[1]Department of Chemistry, North Carolina State University, Raleigh, North Carolina, USA

[2]Joint Department of Biomedical Engineering of University of North Carolina, Chapel Hill and North Carolina State University, Raleigh, North Carolina, USA

[3]Comparative Medicine Institute, North Carolina State University, Raleigh, North Carolina, USA

Correspondence
Ashley C. Brown, Joint Department of Biomedical Engineering, North Carolina State University and University of North Carolina at Chapel Hill, 1001 William Moore Dr, Raleigh, NC 27606, USA.
Email: aecarso2@ncsu.edu

Handling Editor: Dr Robert A. Campbell

Abstract

Background: Fetal fibrinogen is a variant present in neonates. Blood products used in neonates are tailored for adults and do not seamlessly integrate into neonatal clots. Increased sialic acid content has been found in fetal fibrinogen compared with adult fibrinogen. However, the extent or location of sialic acids on fibrinogen remains unknown.

Objectives: To investigate differences in glycosylation and sialic acid content between fetal and adult fibrinogen.

Methods: Glycans were eluted from human cord blood-isolated fetal fibrinogen and commercially available adult fibrinogen using filter-aided *N*-linked glycan separation. A α, B β, and λ chains were isolated using sodium dodecyl sulfate-polyacrylamide gel electrophoresis, and in-gel enzymatic digestion was performed. Infrared matrix-assisted laser desorption electrospray ionization mass spectrometry was used for analysis.

Results: In total, 39 and 22 glycans were detected in fetal and adult fibrinogen, respectively. Fetal fibrinogen glycans were most abundant in the lower molecular weight range <4 kDa. After isolating the Aα, Bβ, and λ chains, increased glycosylation and sialic acid content was found in fetal fibrinogen. Increased glycosylation was detected across all 3 chains, and increased sialic acid content was found in the Bβ chain.

Conclusion: Sialylation in the Bβ chain of fetal fibrinogen supports previous findings showing more knob 'B' interactions occur in fetal fibrinogen than in adult fibrinogen during clot polymerization. This is also the first detection of glycosylation in the Aα chain of fibrinogen. By elucidating the fibrinogen *N*-linked glycome, this study found where sialic acid content differs the most between adult and fetal fibrinogen. This can ultimately be used to develop blood products that are neonatal-compatible.

Tana Palomino and Anastasia Sheridan contributed equally to this work.

KEYWORDS
fetal, fibrinogen, glycan, mass spectrometry, neonate, sialic acid

Essentials

- Neonate bleeding is treated with adult fibrinogen, which can result in ineffective blood clots.
- We investigated sialylation differences between fetal and adult fibrinogen.
- The β chain of fetal fibrinogen had increased levels of sialylated glycans.
- Developing fetal fibrinogen blood products can improve blood clotting during cardiac surgery.

1 | INTRODUCTION

Fibrinogen is an abundant blood protein that is a primary contributor to hemostasis. Once activated by thrombin, this soluble monomer transforms into an insoluble fibrin gel that helps minimize blood loss from injury. Structurally, fibrinogen is a 340-kDa glycoprotein primarily produced in hepatocytes. It consists of 3 paired polypeptide chains (Aα, Bβ, and λ) connected by disulfide bridges in the central N-terminal E domain (Figure 1) [1]. Within the E domain, there are 2 binding sites known as "knobs" located on the Aα and Bβ chains, which become exposed after thrombin binds fibrinogen and cleaves the peptide sequences fibrinopeptide A (FpA) and fibrinopeptide B (FpB), named respectively for the chain on which they reside [2]. In adult fibrinogen, FpA cleavage occurs at a much faster rate than FpB cleavage, leading to fibrin monomer and oligomer formation. Fibrin formation occurs as newly exposed knobs "A" of one fibrin monomer bind with other fibrin monomers via holes "a" located in the distal D regions of the λ chains. These oligomers aggregate laterally as FpB is cleaved leading to knob "B" and hole "b" interactions. These interactions create a dense polymeric fibrin matrix that acts as a provisional scaffold for platelets, growth factors, and other cell types to assist in hemostasis and healing.

Given fibrinogen's central role in hemostasis, adult fibrinogen's structure and function has been studied extensively; however, much remains unknown about neonatal or fetal fibrinogen. Neonates are born with immature hemostatic systems that consist of hyporeactive platelets, lowered intraclot thrombin levels, decreased procoagulant and anticoagulant concentrations, and the presence of a fibrinogen variant called fetal fibrinogen [3,4]. These differences can be attributed to the existing incompatibility issues between adult-based blood products and neonatal patients undergoing surgery [5–7]. Previous studies have shown that fetal fibrinogen creates less stiff and looser clots that degrade faster than adult fibrinogen clots [8]. It has also been shown that during clot polymerization, fetal fibrinogen utilizes significantly more "B-b" knob-hole interactions than adult fibrinogen, which is dominated by "A-a" knob-hole interactions. Structurally, fetal fibrinogen differs from adult fibrinogen in subunit molecular weight and has greater protein phosphorylation and glycosylation [3]. Phosphorylation and glycosylation are classified as posttranslational modifications. Glycosylation, specifically, has been shown to decrease polymerization rate, clot turbidity, and fiber diameter [9]. Glycosylation is the enzyme-mediated addition of a glycan or carbohydrate to a protein or lipid. This process takes place in the endoplasmic reticulum or Golgi apparatus, depending on the type of glycosylation. The 2 main types of glycosylation are *N*-linked, where the sugar molecule is connected to an asparagine (N) residue, and *O*-linked, where the sugar molecule is connected to a serine or threonine (O) [10]. Adult fibrinogen is reported to have 4 *N*-linked glycosylation sites located on the Bβ and λ chains [2]. Sialylation is a specific type of glycosylation that has been shown to have an influence on immune response, aging, and coagulation is sialylation [9].

Sialyation is the addition of a sialic acid group to a monosaccharide residing on a glycoprotein. Adult fibrinogen has ~6 sialic acids located at the *N*-glycosylation sites on the Bβ and λ chains [9]. Sialic acid is a negatively charged glycan residue that can be found on the surface of cells and most proteins [11]. This residue has been shown to influence fibrin clot properties associated with liver disease [12,13]. It was also demonstrated that a reduction in sialic acid caused by fewer galactose residues contributed to faster clot polymerization

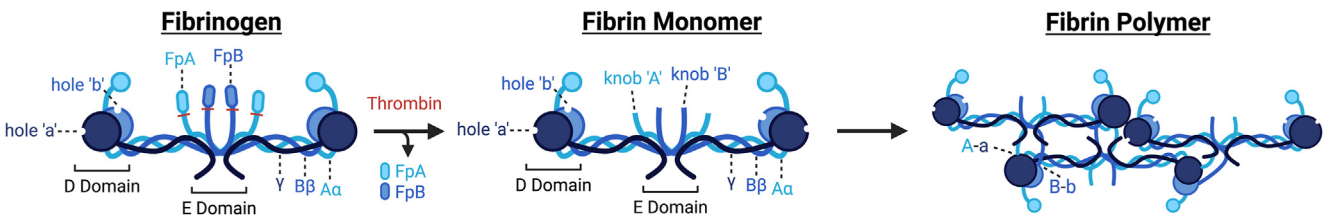

FIGURE 1 Fibrinogen structure and fibrin synthesis. Fibrinogen consists of 3 paired polypeptide chains: α, β, and λ. Thrombin cleaves fibrinogen (red lines) in the E domain, releasing fibrinopeptide FpA and FpB and exposing knob "A" and knob "B." Knobs "A" and knobs "B" of other fibrin monomers bind with holes "a" and holes "b" in the D-domain, thereby creating a fibrin polymer.

[14]. Furthermore, the Brown lab has previously found that fetal fibrinogen has a significantly greater sialic acid concentration than adult fibrinogen [8]; however, the extent and location of this sialylation difference remains unknown. To better elucidate the sialylation difference between adult and fetal fibrinogen, this work used infrared (IR) matrix-assisted laser desorption electrospray ionization (IR-MALDESI) mass spectrometry [15].

IR-MALDESI is one of the ionization mechanisms used for mass spectrometry imaging experiments. A mid-IR laser that fires at the 2970 nm wavelength excites the water molecules present in the sample. The ablated neutral species fly up and are met by an orthogonal electrospray (ESI) plume in which they are ionized in an ESI-like manner. Additionally, IR-MALDESI operates at atmospheric pressure and can detect multiply charged ions. One of the challenges associated with investigating sialic acid by mass spectrometry is its lability. The loss of sialic acid is commonly seen in ionization methods that deposit large amounts of internal energy onto the sample. However, this loss is not observed in IR-MALDESI because the softness of the ionization event is comparable with ESI [16]. As a result, intact sialylated species can be detected and characterized [17–19]. Additionally, the carboxylic acid group on sialic acid indicates a preference for negative ionization mode. Since IR-MALDESI is an ESI-like ionization mechanism, it can ionize sialic acid in its preferred polarity. These benefits allow IR-MALDESI to be an advantageous tool in investigating sialylated glycosylation and was used in this work to uncover sialylation differences in fetal and adult fibrinogen. The experimental workflow used in this study is summarized in Figure 2.

2 | METHODS

2.1 | Fibrinogen sample preparation

Fetal fibrinogen was isolated via ethanol precipitation from pooled human cord blood-recovered plasma in citrate-phosphate-dextrose (ZenBio) [20,21]. Briefly, plasma was mixed with ethanol in a 4:1 ratio and chilled on ice for 20 minutes. The solution was then centrifuged at 1000 *g* for 10 minutes at 4 °C. After the supernatant was removed, the fibrinogen pellet was resuspended with sodium citrate for 5 minutes at 37 °C. Fibrinogen concentration was measured using NanoDrop analysis. Fetal fibrinogen and commercially available adult fibrinogen (Enzyme Research Laboratories) were then resuspended in ultrapure water at 1 mg/mL.

2.2 | *N*-linked glycan cleavage

Filter-aided *N*-linked glycan separation was used to cleave glycans off of fibrinogen samples [22]. Protein (250 μg) was loaded onto a 10 kDa molecular weight cutoff filter, with 100 mM ammonium bicarbonate (ABC) as the buffer solution. Dithiothreitol (DTT) was added to the filter to denature glycoproteins, followed by alkylation with iodoacetamide (IAA). One thousand units of PNGase F (Bulldog Bio) was added to the filter, and the samples were incubated overnight at 37 °C. Samples were dried down using a vacuum desiccator and resuspended in 50 μL water before IR-MALDESI analysis.

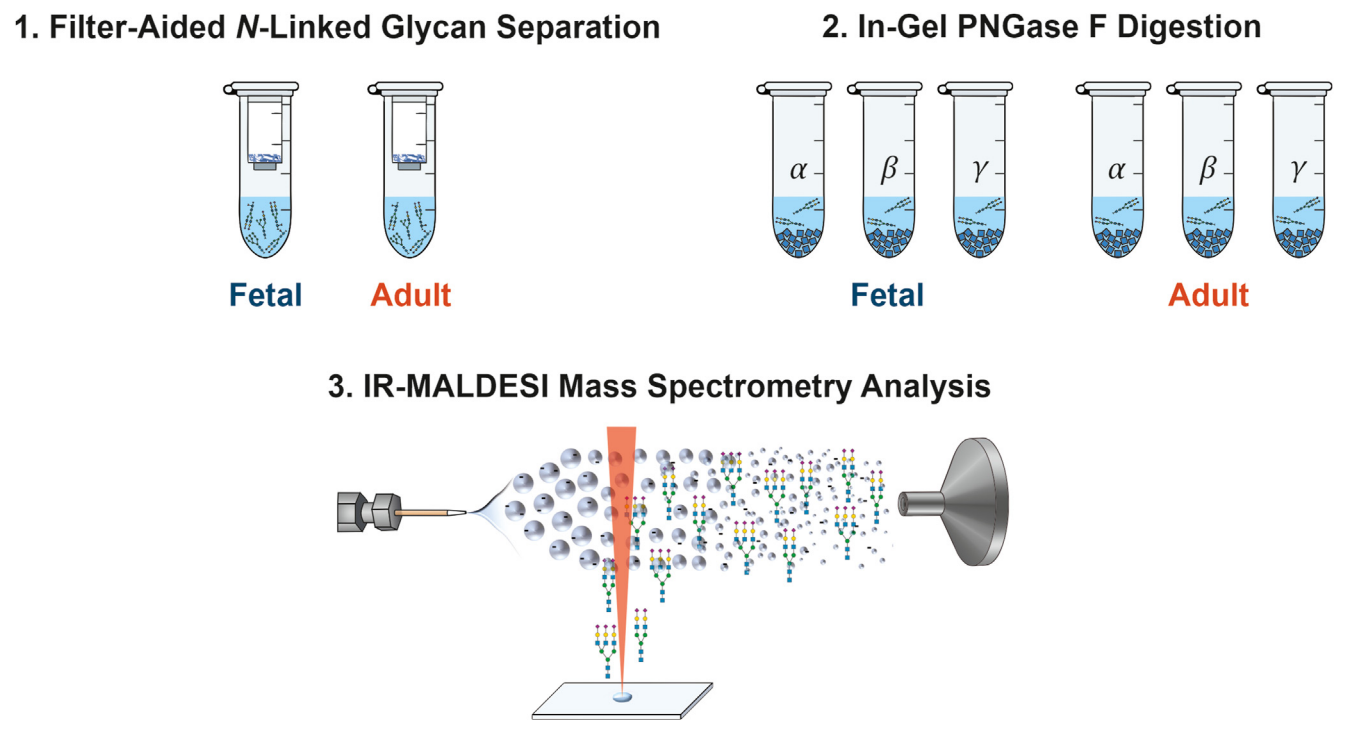

FIGURE 2 Experimental workflow used to investigate differences in glycosylation between fetal and adult fibrinogen. Filter-aided *N*-linked glycan separation was performed with a molecular weight cutoff filter to elute glycans from denatured fibrinogen glycoproteins. In-gel PNGase F digestion cleaved glycans from gel pieces corresponding to the Aα, Bβ, and λ chains of fetal and adult fibrinogen. Infrared matrix-assisted laser desorption electrospray ionization (IR-MALDESI) mass spectrometry was used to ionize and analyze all samples.

2.3 | Aα, Bβ, and λ chain isolation

To isolate Aα, Bβ, and λ chains from adult and fetal fibrinogen, sodium dodecyl sulfate-polyacrylamide gel electrophoresis (SDS-PAGE) was performed on 8% Novex Tris-Glycine WedgeWell Mini Gels (Invitrogen) in conjunction with a Mini Gel Tank (Invitrogen) and PowerPac HC power supply (Bio-Rad). Sample reduction and SDS-PAGE were carried out according to manufacturer recommendations (Novex, Tris-Glycine Mini Gels; WedgeWell Format; Thermo Fisher). Each lane was loaded with 15 μg protein. Following gel electrophoresis, bands were stained using SimplyBlue SafeStain (Invitrogen) and imaged. Densitometry was performed on ImageJ to estimate protein amount per band. SDS-PAGE and densitometry measurements are shown in Figure 3.

2.4 | In-gel enzymatic digestion

The Aα, Bβ, and λ chain gel bands in fetal and adult fibrinogen were excised and cut into small pieces before performing in-gel PNGase F enzymatic digestion. Both fetal Aα bands present in the gel were isolated together to represent total fetal Aα glycosylation. Gel pieces were destained using 50:50 100 mM ABC:acetonitrile (ACN), followed by 100% ACN. The gels were incubated with DTT and 100 mM ABC at 56 °C for 30 minutes. After cooling to room temperature and removing DTT solution, ACN was added to dehydrate the gel pieces and incubated at room temperature for 15 minutes. After ACN was removed, IAA and ABC were added to the gel pieces and incubated at 37 °C for 1 hour. Once the IAA was removed, another dehydration step using ACN was performed. After removal of ACN, 1000 units of PNGase F were added to the gel pieces and incubated overnight at 37 °C. Extracted glycan solutions were transferred to a new vial. The gel pieces were dehydrated using ACN and incubated at room temperature for 10 minutes before transferring the ACN to the new vial. Rehydration of the gel pieces was performed by adding ABC and incubating at room temperature for 10 minutes. The ABC solution was then transferred to the new vial, and the rehydration–dehydration cycle was performed 2 more times. The extracted glycan solution was then dried down using a vacuum desiccator and resuspended in 50 μL of water before analyzing by IR-MALDESI.

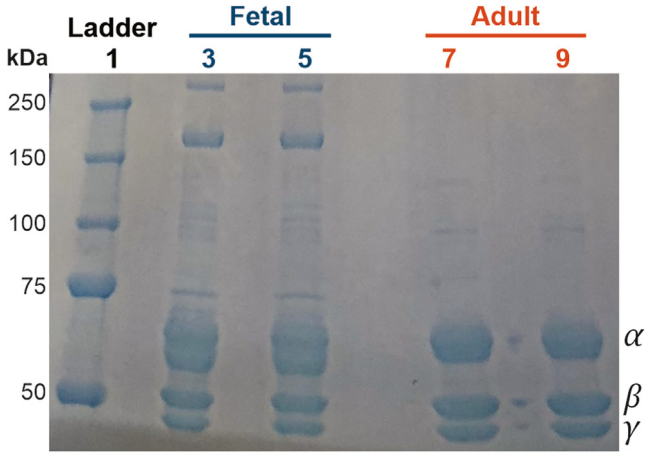

	Fetal		Adult	
Chain	Lane 3	Lane 5	Lane 7	Lane 9
α	6.8904	6.6778	7.6558	6.5015
β	2.7185	2.9287	4.4507	5.3913
γ	1.5640	1.5785	2.8935	3.1071

FIGURE 3 Sodium dodecyl sulfate-polyacrylamide gel isolating Aα, Bβ, and λ chains in fetal and adult fibrinogen (top). Densitometry measurements corresponding to each chain in fetal and adult fibrinogen (bottom).

2.5 | IR-MALDESI mass spectrometry and data analysis

Due to the softness of the ionization source, IR-MALDESI can ionize sialylated *N*-linked glycans without chemical derivatization. IR-MALDESI uses an infrared laser (JGM Associates) that fires at the 2.97 μm wavelength to excite the water molecules present in the sample and matrix. Six pulses per burst were used and achieved a laser energy of 2 mJ per voxel. IR-MALDESI was coupled to an Orbitrap Exploris 240 mass spectrometer (Thermo Fisher Scientific). Mass calibration was performed each day of experiments. The ESI solvent consisted of 50% ACN with 1 mM acetic acid. A stable ESI plume was achieved with 3000 V and a flow rate of 1 μL/min. Five microliters of sample was pipetted onto a hydrophobic slide and directly analyzed by IR-MALDESI. Raw mass spectra were converted from *m/z* ratios to monoisotopic mass. Masses were uploaded into GlycoMod to determine potential glycan compositions, and annotations were confirmed by GlyConnect, an experimental database [23,24]. The relative abundance of the glycans was obtained from the raw mass spectra and divided by the amount of protein per gel band in micrograms to obtain ions per second per microgram. The number of sialic acids on each glycan was determined and multiplied by the relative abundance of the glycan to obtain total sialic acid content as sialic acids per second per microgram. Percentage difference calculations were performed to determine the degree of the differences between fetal and adult fibrinogen.

3 | RESULTS

3.1 | Characteristics of glycosylation in fetal and adult fibrinogen

A total of 38 glycans were detected in fetal fibrinogen, and 22 glycans were detected in adult fibrinogen. All glycans were detected as multiply charged species within a 2.5 ppm mass measurement accuracy. Nineteen glycans were shared between fetal and adult fibrinogen. Three glycans were exclusive to adult fibrinogen, and 19 glycans were exclusive to fetal fibrinogen (Figure 4A). All detected glycans are

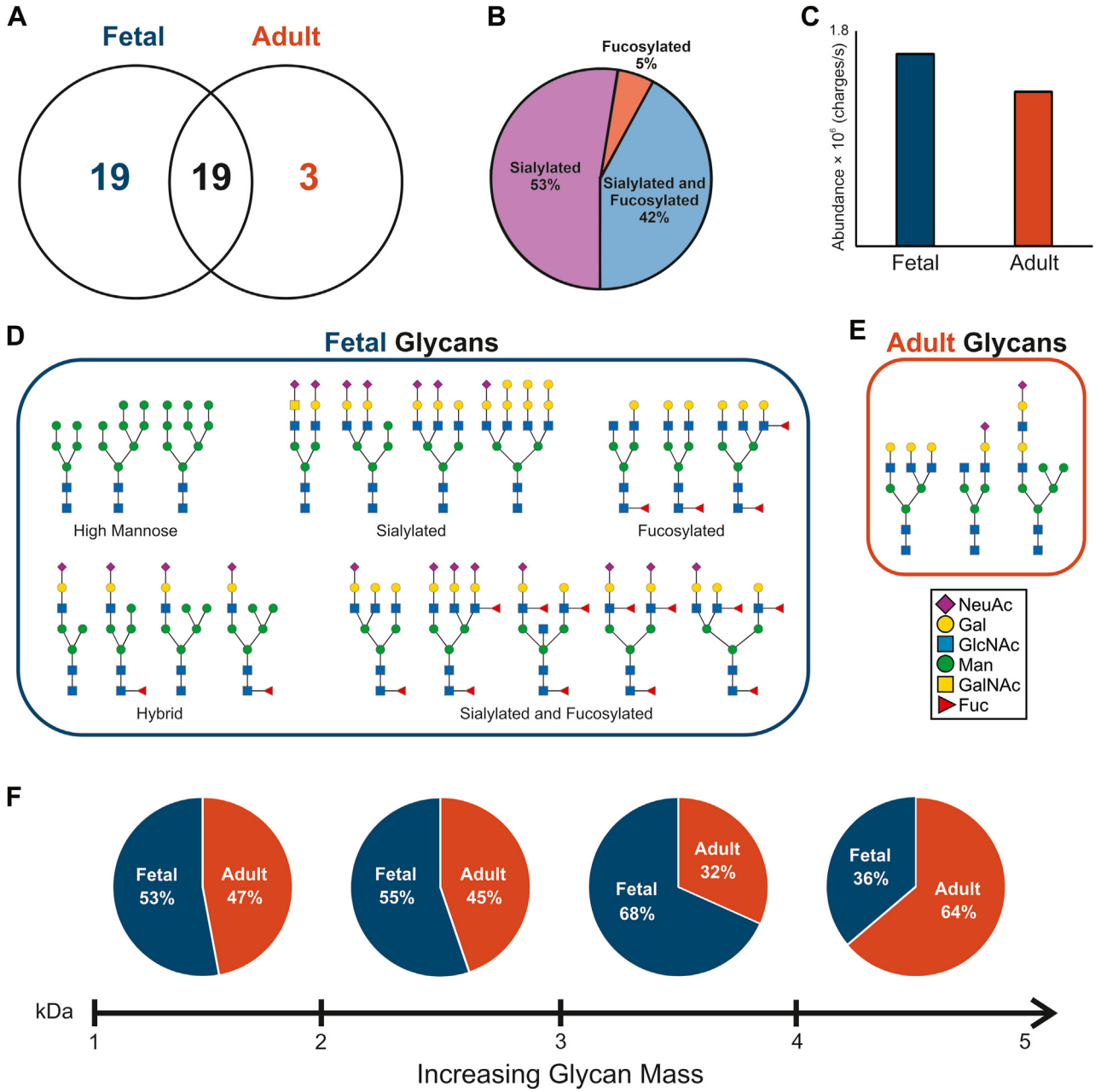

FIGURE 4 (A) Venn diagram of glycans detected in fetal and adult fibrinogen. (B) Characteristics of the common glycans shared between fetal and adult fibrinogen. (C) Total relative abundance of fetal and adult glycans. (D) Putative structures of *N*-linked glycans only detected in fetal fibrinogen. (E) Putative structures of *N*-linked glycans only detected in adult fibrinogen. (F) Size trends in glycans detected in both fetal and adult fibrinogen. Fetal fibrinogen has a higher abundance of small to mid-size glycans (1-4 kDa) compared with adult fibrinogen. Adult fibrinogen has a higher abundance of large glycans (>4 kDa) compared with fetal fibrinogen. Glycan structures are represented using Symbol Nomenclature for Glycans. Fuc, fucose; Gal, galactose; GalNAc, *N*-acetylgalactosamine; GlcNAc, *N*-acetylglucosamine; Man, mannose; NeuAc, *N*-acetylneuraminic acid.

listed in Supplementary Tables 1 to 3. The 19 common glycans were mostly sialylated glycans, a few fucosylated glycans, and several sialylated and fucosylated glycans (Figure 4B). The total glycan abundance was higher in fetal fibrinogen than in adult fibrinogen, as shown in Figure 4C, likely due to the additional number of glycans detected in fetal fibrinogen. Glycan structures detected only in fetal fibrinogen are shown in Figure 4D. High mannose, hybrid, and complex structures were detected, and the complex and hybrid structures included sialylated and fucosylated glycans. High mannose glycans were only detected in fetal fibrinogen. Glycan structures exclusive to adult fibrinogen are shown in Figure 4E. Two complex glycans and 1 hybrid glycan with a polylactosamine extension were detected. Investigation into the glycans detected in both fetal and adult fibrinogen within a specific mass range revealed unique trends. As shown in

Figure 4F, fetal fibrinogen glycans had a greater abundance of glycans within the 1 to 4 kDa glycan mass range, particularly within the 3 to 4 kDa mass range. Glycans in the 4 to 5 kDa mass range were most abundant in adult fibrinogen.

3.2 | Aα, Bβ, and λ chain glycosylation

Four total glycans were detected in the SDS-PAGE analysis in both fetal and adult fibrinogen. Raw mass spectra of the detected glycans in each chain within fetal and adult fibrinogen is shown in Figure 5. All glycans were detected as multiply charged species within a 2.5 ppm mass measurement accuracy. Three glycans were detected in the Aα chain, 2 in the Bβ chain, and 4 in the λ chain. The 4 glycans consisted of mono-, di-, tri-, and tetrasialylated glycans. Di-, tri-, and tetrasialylated glycans were detected in the Aα chain, mono- and disialylated glycans were detected in the Bβ chain, and mono-, di-, tri-, and tetrasialylated glycans were detected in the λ chain (Figure 6). Certain glycans were common among some of the chains, and a Euler diagram depicting shared glycans between each chain is shown in Figure 6.

3.3 | Differences in *N*-glycosylation and sialic acid content

The relative abundance of ions per microgram of protein was determined using densitometry. In the Aα chain, a higher relative abundance of disialylated glycans was found in fetal fibrinogen, and adult fibrinogen had a higher relative abundance of tri- and tetrasialylated glycans (Figure 7A). In the Bβ chain, fetal fibrinogen had a higher relative abundance of both detected glycans than adult fibrinogen (Figure 7A). Finally, in the λ chain, fetal fibrinogen had a higher relative abundance of the mono- and disialylated glycans, and adult fibrinogen had a higher relative abundance of the tri- and tetrasialylated glycans (Figure 7A). A summary of total glycosylation within each chain is presented in Figure 7B. Larger amounts of glycosylation was detected in fetal fibrinogen across all chains. The percentage differences for the Aα, Bβ, and λ chains were 34%, 41%, and 28%, respectively. Interestingly, the Bβ chain had the largest difference in total glycosylation between fetal and adult fibrinogen (Figure 7B).

Total sialic acid content between fetal and adult fibrinogen chains was investigated by multiplying the relative abundance (ions per second per microgram) by the number of sialic acids present on the glycan to obtain sialic acids per second per microgram. Sialic acid content resulting from each glycan within each chain is depicted in Figure 8A. The majority of sialic acid content across all 3 chains came from the biantennary disialylated glycan. However, a significant portion of sialic acid content present in adult fibrinogen came from tri- and tetrasialylated glycans. A summary of sialic acid content within each chain is shown in Figure 8B. Comparable sialic content was observed in the Aα and λ chains between fetal and adult fibrinogen. The percentage differences were 5.5% and 0.8% for the Aα and λ chains, respectively. Higher sialic acid content was observed in the Bβ chain in fetal fibrinogen compared with adult fibrinogen (Figure 8B). The percentage difference between fetal and adult Bβ chain sialic acid content was 44%, indicating a significant increase in sialylation in the Bβ chain of fetal fibrinogen. Overall, fetal fibrinogen had greater abundances of both total glycosylation and sialic acid content due to the significant increase in glycosylation within the Bβ chain.

4 | DISCUSSION

Fibrinogen samples were prepared using filter-aided *N*-linked glycan separation to cleave *N*-linked glycans off fibrinogen. Glycans were then directly analyzed by IR-MALDESI, in which an abundance of *N*-linked glycans was detected in fetal and adult fibrinogen. High mannose glycans were only detected in purified fetal fibrinogen. This is consistent with previous studies that found higher levels of high mannose glycans in neonate samples [25]. Because *N*-linked glycans follow a non-template synthesis, the spatiotemporal distribution of enzymes that can act upon the protein to synthesize a glycan can vary based on genetics, age, environmental conditions, and more [26]. High mannose glycans are precursor oligosaccharides to complex and hybrid glycans, suggesting that the abundance of certain glycotransferases is rather low in neonates compared with adults. Fetal fibrinogen also had a higher number of *N*-linked glycans detected. The high abundance of fetal glycans within the 3 to 4 kDa range indicates that these glycans may play a role in neonatal blood clotting. The high abundance of adult glycans in the 4 to 5 kDa mass range indicate a significant amount of glycan processing in the Golgi that is not fully developed in neonates. These results demonstrated clear differences in glycosylation between fetal and adult fibrinogen and motivated a deeper investigation into the location of these glycans within fibrinogen.

To investigate glycosylation within each fibrinogen chain, SDS-PAGE was performed to separate the Aα, Bβ, and λ subunits. After band excision and in-gel PNGase F digestion, glycans were analyzed by IR-MALDESI mass spectrometry. Notably, to our knowledge, this is the first study to detect glycosylation within the Aα chain. Although the relative abundance of glycans was an order of magnitude lower than the other fibrinogen chains, 3 glycans were confidently detected and confirmed by high mass measurement and spectral accuracy. Prior research only detected mono-, di-, and trisialylated glycans in fibrinogen [27]. However, in this work, we report a tetrasialylated glycan detected in the Aα and λ chains. This glycan was more abundant in adult fibrinogen compared with fetal fibrinogen, which is consistent with the findings from the direct protein analysis in which larger glycans tended to be more abundant in adult fibrinogen. Glycans with 2 branches (mono- and disialylated) were always more abundant in fetal fibrinogen. Overall, these size trends present in both analyses indicate that larger and more processed glycans are more common during adulthood.

While specific impact of sialic acid on clot polymerization is not fully understood, multiple studies have shown that sialic acid inhibits polymerization rate [8,28]. One explanation for this inhibition is electrostatic repulsion due to the negatively charged carboxylic acid

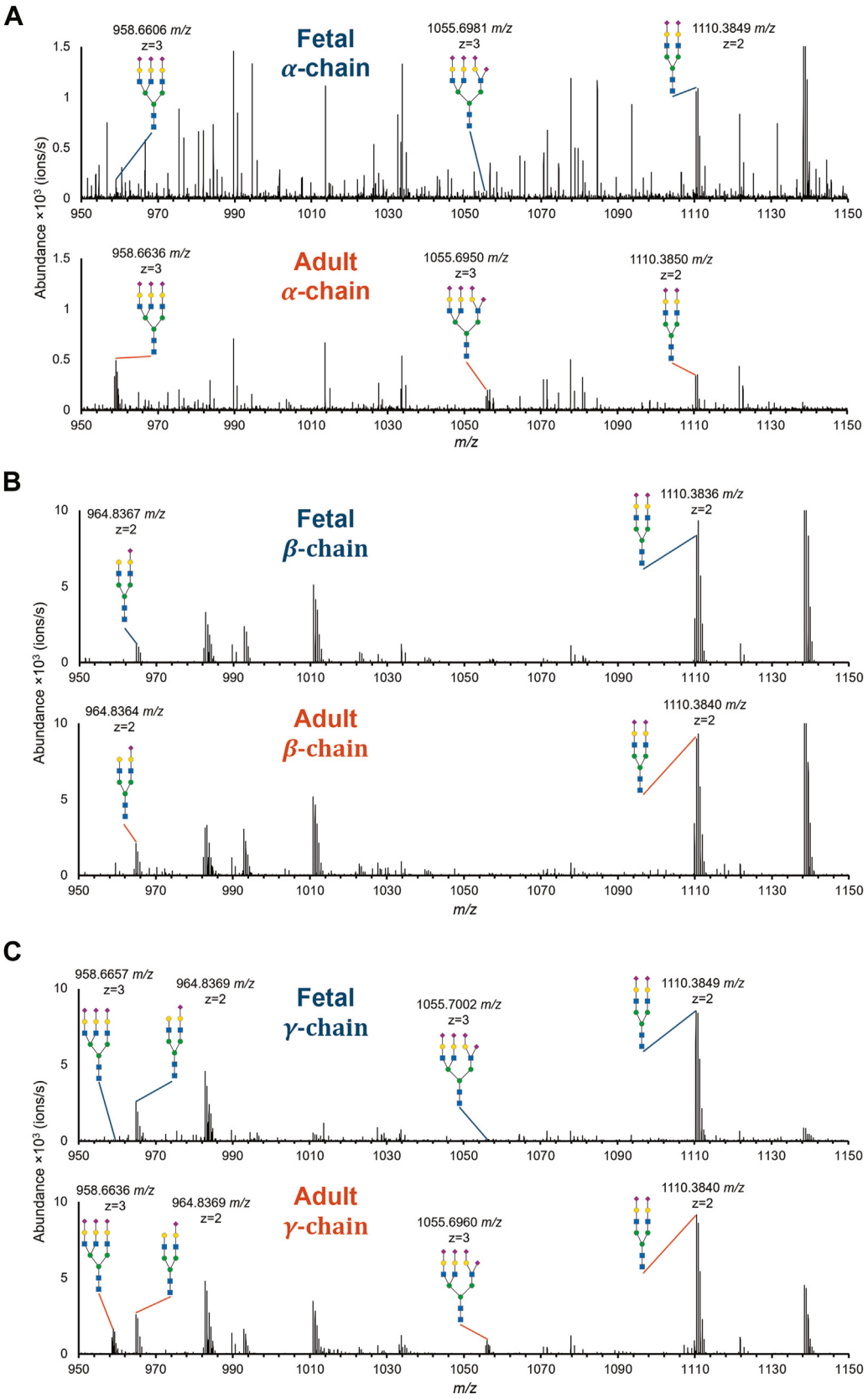

FIGURE 5 Raw mass spectra of the A α, B β, and λ fibrinogen chains in both fetal and adult fibrinogen. (A) A α chain mass spectra of fetal and adult fibrinogen. (B) Bβ chain mass spectra of fetal and adult fibrinogen. (C) λ chain mass spectra of fetal and adult fibrinogen.

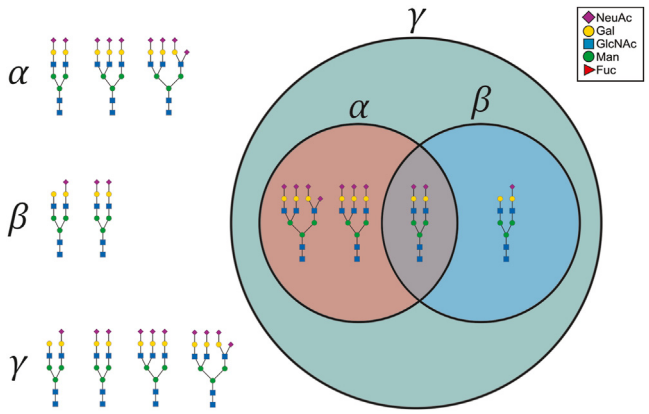

FIGURE 6 Glycan structures detected in the Aα, Bβ, and λ chains (left). Euler diagram depicting common sialylated glycans between each chain (right). Fuc, fucose; Gal, galactose; GlcNAc, *N*-acetylglucosamine; Man, mannose; NeuAc, *N*-acetylneuraminic acid.

functional group present on sialic acid. Normally, the negative charge can be neutralized by calcium. However, in elevated levels of sialic acid, there is not enough calcium for the neutralization, and polymerization is inhibited. Other studies have shown that sialic acid not only impacts fibrin monomer polymerization but also the latter steps of crosslinking fibrin monomer into a cross-linked fibrin matrix [29]. It is hypothesized that sialic acid influences factor XIII crosslinking mechanisms, thereby reducing clot turbidity. These theories support previous studies that showed heavily sialylated fetal fibrinogen has lower clot polymerization rates and clot turbidity than adult fibrinogen [8]. Furthermore, this study showed that fetal fibrinogen has significantly more knob 'B' interactions than knob 'A' interactions during clot polymerization. This is directly supported by the findings in this work demonstrating increased sialic acid content in the Bβ chain of fetal fibrinogen compared with adult fibrinogen. However, the specifics for how sialic acid promotes knob "B" interactions remain unknown.

This work has expanded upon previous findings that show that adult and fetal fibrinogen are structurally and functionally different. Specifically, this analysis has elucidated where sialic acid residues differ the most between adult and fetal fibrinogen, which can be used to better understand functional differences between the 2 molecules. Understanding these differences is critical to developing therapies to treat bleeding in infants without the thrombotic risks currently associated with administration of adult blood products to neonates requiring transfusion. More specifically, the findings presented in this work build a foundation for future studies focused on making adult fibrinogen more fetal-like via chemical modification, thereby creating a concentrated fibrinogen therapeutic that is adult-based and neonatal-compatible. This type of therapeutic would not only mitigate blood compatibility issues between adult-based blood products and neonates but would also circumvent any ethical and availability concerns with the use of neonatal-derived blood products. To develop such a therapeutic, the specific role of sialic acid in clot polymerization needs to be understood. Future studies will be conducted to elucidate this information, use it to modify adult fibrinogen to be more fetal-like, and compare it with clinically available adult fibrinogen concentrate.

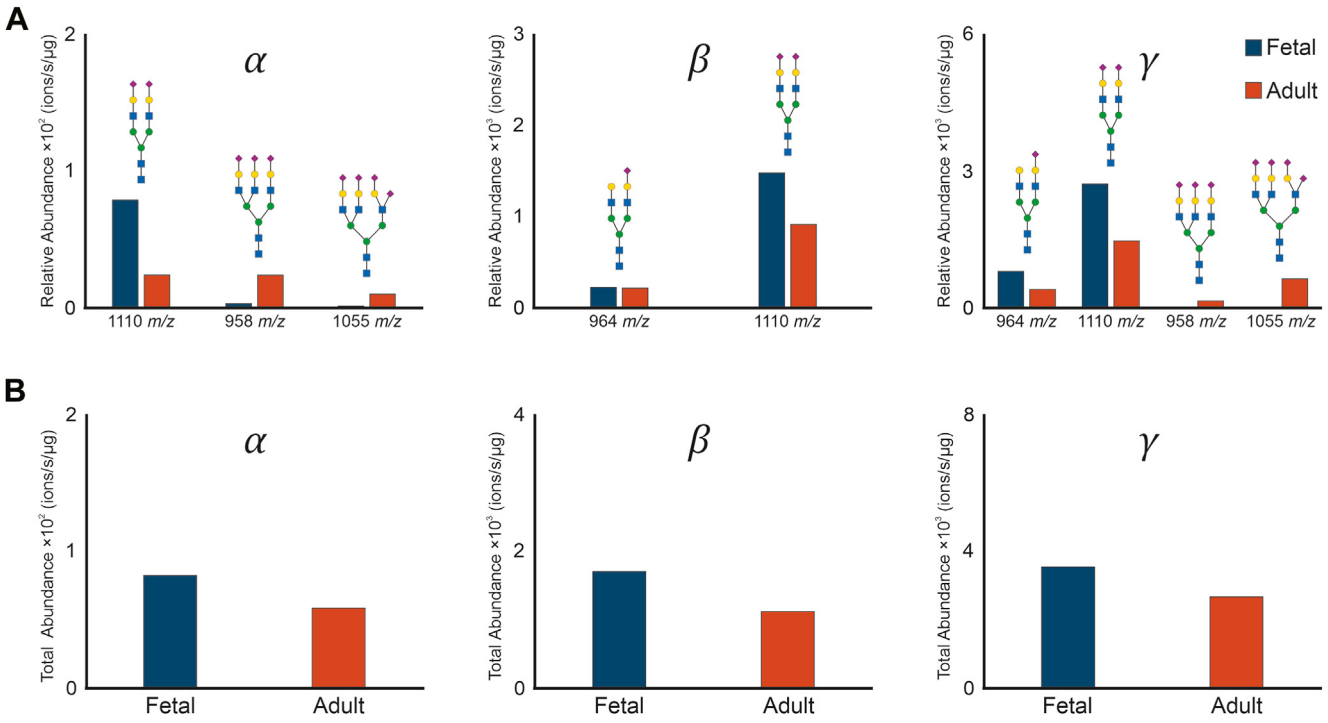

FIGURE 7 (A) Relative abundance (ions/s/μg) of each detected *N*-linked glycan in each chain. The biantennary disialylated glycan (1110 *m/z*) was most abundant in fetal fibrinogen across each chain. (B) Total relative abundance of *N*-glycosylation across each chain in fetal and adult fibrinogen. Higher levels of glycosylation were observed in each chain of fetal fibrinogen compared with adult fibrinogen.

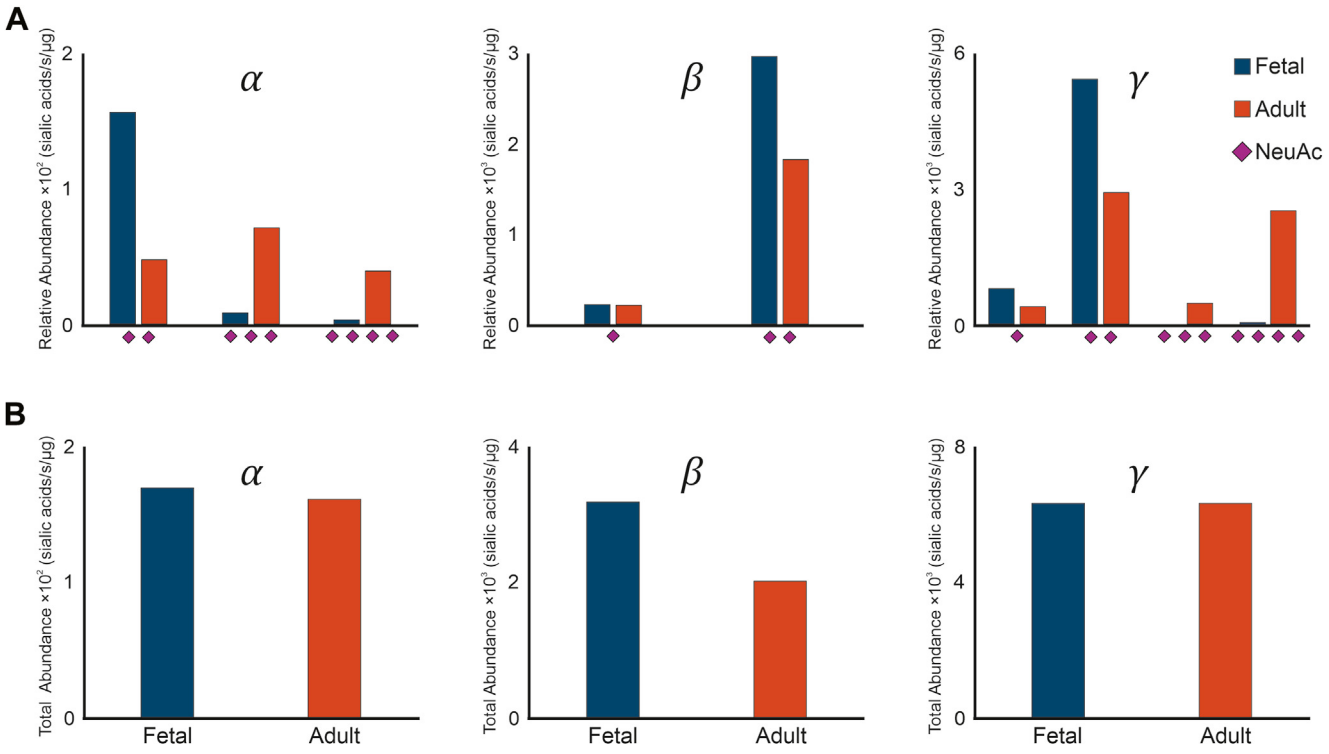

FIGURE 8 (A) Relative abundance of sialic acids (sialic acids/s/μg) from each sialylated glycan in each chain. The majority of sialic acid content resulted from the biantennary disialylated glycan (1110 *m/z*), which was the most abundant glycan across all chains. (B) Total abundance of sialic acid content across each chain in fetal and adult fibrinogen. Comparable levels of sialic acid content were observed in the Aα and λ chains and increased sialic acid content was observed in the Bβ chain in fetal fibrinogen compared with adult fibrinogen. NeuAc, *N*-acetylneuraminic acid.

5 | CONCLUSION

Fetal fibrinogen *N*-glycosylation has a higher relative abundance of lower molecular weight glycans and higher sialic acid content than adult fibrinogen. Glycans conjugated to the Bβ chain of fetal fibrinogen had significantly higher sialic acid content, supporting previous findings in which more knob 'B' interactions occur in fetal fibrinogen compared with adult fibrinogen during clot polymerization. This is also the first study to detect glycosylation in the Aα chain. Overall, we elucidated and expanded the fibrinogen *N*-linked glycome and present important differences in sialic acid content between each of the 3 subunits. Future work includes further probing the structural differences between adult and fetal fibrinogen through mass spectrometry imaging of blood clots.

ACKNOWLEDGMENTS

All mass spectrometry measurements were made in the Molecular Education, Technology and Research Innovation Center (METRIC) at North Carolina State University.

FUNDING

The authors gratefully acknowledge the financial support received from the National Institutes of Health (R01GM087964; T32GM133366), NSF (DGE-213700; EBMS-2211404), and AHA and North Carolina State University.

AUTHOR CONTRIBUTIONS

T.P. performed experiments, analyzed results, and wrote the paper. A.S. processed samples, performed experiments, and wrote the paper. D.M. assisted in research design and revised the paper. A.B. designed and supervised the study and revised the paper.

RELATIONSHIP DISCLOSURE

A.C.B. is cofounder of Selsym Biotech, Inc, a start-up company focused on developing hemostatic therapies. T.V.P., A.S., and D.C.M. declare no conflicts of interest.

ORCID

Ashley C. Brown https://orcid.org/0000-0001-6995-1785

X

Ashley C. Brown @brownlab_ncsu

REFERENCES

[1] Weisel JW, Litvinov RI. Fibrin formation, structure and properties. *Subcell Biochem*. 2017;82:405–56.

[2] Geer CB, Tripathy A, Schoenfisch MH, Lord ST, Gorkun OV. Role of 'B-b' knob-hole interactions in fibrin binding to adsorbed fibrinogen. *J Thromb Haemost*. 2007;5:2344–51.
[3] Ignjatovic V, Mertyn E, Monagle P. The coagulation system in children: developmental and pathophysiological considerations. *Semin Thromb Hemost*. 2011;37:723–9.
[4] Revel-Vilk S. The conundrum of neonatal coagulopathy. *Hematology Am Soc Hematol Educ Program*. 2012;2012:450–4.
[5] Faraoni D, Emani S, Halpin E, Bernier R, Emani SM, DiNardo JA, et al. Relationship between transfusion of blood products and the incidence of thrombotic complications in neonates and infants undergoing cardiac surgery. *J Cardiothorac Vasc Anesth*. 2017;31:1943–8.
[6] Solomon C, Rahe-Meyer N, Sørensen B. Fibrin formation is more impaired than thrombin generation and platelets immediately following cardiac surgery. *Thromb Res*. 2011;128:277–82.
[7] Manlhiot C, Menjak IB, Brandão LR, Gruenwald CE, Schwartz SM, Sivarajan VB, et al. Risk, clinical features, and outcomes of thrombosis associated with pediatric cardiac surgery. *Circulation*. 2011;124:1511–9.
[8] Nellenbach K, Kyu A, Guzzetta N, Brown AC. Differential sialic acid content in adult and neonatal fibrinogen mediates differences in clot polymerization dynamics. *Blood Adv*. 2021;5:5202–14.
[9] de Vries JJ, Snoek CJM, Rijken DC, de Maat MPM. Effects of post-translational modifications of fibrinogen on clot formation, clot structure, and fibrinolysis. *Arterioscler Thromb Vasc Biol*. 2020;40:554–69.
[10] Rachmilewitz J. Glycosylation: an intrinsic sign of "danger". *Self Nonself*. 2010;1:250–4.
[11] Varki A. Sialic acids in human health and disease. *Trends Mol Med*. 2008;14:351–60.
[12] Lisman T, Ariëns RAS. Alterations in fibrin structure in patients with liver diseases. *Semin Thromb Hemost*. 2016;42:389–96.
[13] Martinez J, MacDonald KA, Palascak JE. The role of sialic acid in the dysfibrinogenemia associated with liver disease: distribution of sialic acid on the constituent chains. *Blood*. 1983;61:1196–202.
[14] Brennan SO. Variation of fibrinogen oligosaccharide structure in the acute phase response: possible haemorrhagic implications. *BBA Clin*. 2015;3:221–6.
[15] Bagley MC, Garrard KP, Muddiman DC. The development and application of matrix assisted laser desorption electrospray ionization: the teenage years. *Mass Spectrom Rev*. 2023;42:35–66.
[16] Tu A, Muddiman DC. Internal energy deposition in infrared matrix-assisted laser desorption electrospray ionization with and without the use of ice as a matrix. *J Am Soc Mass Spectrom*. 2019;30:2380–91.
[17] Pace CL, Angel PM, Drake RR, Muddiman DC. Mass spectrometry imaging of *N*-linked glycans in a formalin-fixed paraffin-embedded human prostate by infrared matrix-assisted laser desorption electrospray ionization. *J Proteome Res*. 2022;21:243–9.
[18] Palomino TV, Muddiman DC. Predicting sialic acid content of *N*-linked glycans using the isotopic pattern of chlorine. *J Am Soc Mass Spectrom*. 2023;34:1392–9.
[19] Samal J, Palomino TV, Chen J, Muddiman DC, Segura T. Enhanced detection of charged *N*-glycans in the brain by infrared matrix-assisted laser desorption electrospray ionization mass spectrometric imaging. *Anal Chem*. 2023;95:10913–20.
[20] Qiu LL, Levinson SS, Keeling KL, Elin RJ. Convenient and effective method for removing fibrinogen from serum specimens before protein electrophoresis. *Clin Chem*. 2003;49:868–72.
[21] Dietrich M, Heselhaus J, Wozniak J, Weinandy S, Mela P, Tschoeke B, et al. Fibrin-based tissue engineering: comparison of different methods of autologous fibrinogen isolation. *Tissue Eng Part C Methods*. 2013;19:216–26.
[22] Hecht ES, McCord JP, Muddiman DC. A quantitative glycomics and proteomics combined purification strategy. *J Vis Exp*. 2016;109:e53735.
[23] Alocci D, Mariethoz J, Gastaldello A, Gasteiger E, Karlsson NG, Kolarich D, et al. GlyConnect: glycoproteomics goes visual, interactive, and analytical. *J Proteome Res*. 2019;18:664–77.
[24] Cooper CA, Gasteiger E, Packer NH. GlycoMod–a software tool for determining glycosylation compositions from mass spectrometric data,". *Proteomics*. 2001;1:340–9.
[25] Contessotto P, Ellis BW, Jin C, Karlsson NG, Zorlutuna P, Kilcoyne M, et al. Distinct glycosylation in membrane proteins within neonatal versus adult myocardial tissue. *Matrix Biol*. 2020;85–86:173–88.
[26] Varki A, Esko JD, Colley KJ. Cellular organization of glycosylation. In: Varki A, Cummings RD, Esko JD, Freeze HH, Stanley P, Bertozzi CR, et al., eds. *Essentials of glycobiology*. 2nd ed. Cold Spring Harbor, NY: Cold Spring Harbor Laboratory Press; 2009.
[27] Adamczyk B, Struwe WB, Ercan A, Nigrovic PA, Rudd PM. Characterization of fibrinogen glycosylation and its importance for serum/plasma *N*-glycome analysis. *J Proteome Res*. 2013;12:444–54.
[28] Dang CV, Shin CK, Bell WR, Nagaswami C, Weisel JW. Fibrinogen sialic acid residues are low affinity calcium-binding sites that influence fibrin assembly. *J Biol Chem*. 1989;264:15104–8.
[29] Okude M, Yamanaka A, Morimoto Y, Akihama S. Sialic acid in fibrinogen: effects of sialic acid on fibrinogen-fibrin conversion by thrombin and properties of asialofibrin clot. *Biol Pharm Bull*. 1993;16:448–52.

SUPPLEMENTARY MATERIAL

The online version contains supplementary material available at https://doi.org/10.1016/j.rpth.2024.102618